

## Low-temperature transport of magnetic excitons in the quasi-one-dimensional antiferromagnet $\text{CsMnCl}_3 \cdot 2\text{H}_2\text{O}$ doped with $\text{Cu}^{2+}$ ions

V. Eremenko, V. Karachevtsev, V. Shapiro, and V. Slavin

*Institute for Low Temperature Physics and Engineering 47, Lenin Avenue, 310164, Kharkov, Ukraine*

(Received 19 September 1995; revised manuscript received 20 December 1995)

The emission decay kinetics and relative quantum yields of exciton luminescence of  $\text{Cu}^{2+}$ -doped (3%) quasi-one-dimensional antiferromagnetic crystals  $\text{CsMnCl}_3 \cdot 2\text{H}_2\text{O}$  have been studied in the temperature range from 4.2 to 77 K. The experimental emission decay curves have been approximated by the calculated curves obtained using computer simulation of incoherent excitons motion. The model assumes a slow interchain hopping process and a rapid intrachain migration of excitons. Exciton hopping ( $W$ ) and trapping ( $U$ ) rates at 4.2–77 K have been defined. A decrease of both  $U$  and  $W$  rates has been observed with a temperature lowering. The proposed model of exciton migration and trapping considered excitation passing potential barriers between  $\text{Mn}^{2+}$ - $\text{Mn}^{2+}$  and  $\text{Mn}^{2+}$ - $\text{Cu}^{2+}$  ions. To describe the deviation of  $U(T)$  and  $W(T)$  dependences from the Arrhenius law we suppose that excitons pass barriers by both hopping over it and tunneling. The energies and shapes of the barriers have been estimated. The tunneling processes were taken into account while determining the barriers energy. The role of both the exciton-phonon interaction in  $\text{CsMnCl}_3 \cdot 2\text{H}_2\text{O}$  and the spin forbiddenness of the low-temperature ( $T \leq 30$  K) exciton migration along a chain due to the antiferromagnetic spin ordering has been discussed. [S0163-1829(96)04322-6]

### I. INTRODUCTION

Exciton migration in quasi-one-dimensional (q-1D) antiferromagnets (AFM's) is most completely studied experimentally in  $(\text{CH}_3)_4\text{NMnCl}_3$ ,<sup>1,2</sup>  $\text{CsMnCl}_3 \cdot 2\text{H}_2\text{O}$  (CMC),<sup>3</sup> and  $\text{CsMnBr}_3$  (Ref. 4) crystals. The luminescence studies showed that fast exciton transport in these AFM's was observed above 50 K. A sufficiently strong exciton-phonon interaction in these crystals (for CMC see Ref. 5) seems to be one of the essential reasons of exciton migration freezing at low temperatures. At  $T > 50$  K the exciton motion is considered to be incoherent hops between adjacent ions of  $\text{Mn}^{2+}$ .<sup>1-4</sup> Traps for excitons are often used in luminescence investigations as a sensitive probe for controlling mobility of excitations in crystals. In AFM's different dopants ( $\text{Cu}^{2+}$ ,  $\text{Co}^{2+}$ ,  $\text{Ni}^{2+}$ ,  $\text{Fe}^{2+}$ ,  $\text{Cr}^{2+}$ ,  $\text{Er}^{3+}$ ,<sup>1-6</sup> etc.) appear to be traps for excitons. The exciton or trap emission decay kinetics is recorded in experimental investigations. This method is most commonly used in the studies of q-1D or one-dimensional (1D) systems since it allows us to determine the migration parameters (exciton hopping  $W$ , and trapping  $U$ , rates) directly from fitting the emission decay curves.

The exciton motion over a 1D chain with efficient ( $U \geq W$ ) and inefficient ( $U < W$ ) trapping has been considered in many theoretical models.<sup>7-14</sup> The q-1D character of exciton transport has been taken into account by the Monte Carlo simulation of these processes in crystals.<sup>15,16</sup> All these models have been used for fitting the experimental curves of exciton emission decay in AFM's. It has been established that in the above-mentioned q-1D AFM's the value of  $W$  increases from  $10^7 - 10^8 \text{ s}^{-1}$  at 77 K to  $10^{11} - 10^{12} \text{ s}^{-1}$  at 250 K.<sup>1-4</sup>

The model of coherent excitons was used to approximate the emission decay curves of  $\text{CsMnCl}_3 \cdot 2\text{D}_2\text{O}$  crystals doped with  $\text{Co}^{2+}$  at 2 K.<sup>17</sup> The coherent motion of excitons

in q-1D AFM crystals was not considered before. The temperature range of 4.2–50 K where the exciton transport topology may be changed from the coherent to incoherent type is of extreme interest and presents a fairly complicated field of investigation. The main difficulties are connected with a choice of a migration model (coherent or hopping) to approximate the emission decay curves. It should be noted that the number of experimental methods defining the type of exciton motion is extremely limited (e.g., EPR in the excited state or a shape of the zero-phonon line were used to determine the triplet exciton transport topology in molecular crystals<sup>18</sup>) and often inapplicable to AFM crystals. Difficulties in both the computer simulation and theoretical analysis are due to a lack of common model describing coherent, incoherent or partially coherent excitons.

In q-1D AFM crystals, besides the strong exciton-phonon interaction, exciton transport is appreciably affected by the AFM spin correlation in chains that occurs at low temperatures (e.g.,  $T < 20 - 30$  K for CMC). As a result, exciton migration has to slow down since the spins of the neighboring  $\text{Mn}^{2+}$  ions (in chains) are directed opposite to each other and a spin block against motion takes effect. A temperature increase leads to the loss of the spin mutual correlation and exciton migration along 1D chains is activated.

In this temperature range the role of magnetic subsystem also manifests itself in an increase of relative quantum yields of the exciton luminescence with a temperature rise as it is the case in undoped CMC crystals.<sup>19</sup> This is due to an additional mechanism of the emission involving thermoactivated magnons.

In the present paper we have studied the emission decay kinetics and relative quantum yields of exciton luminescence of  $\text{Cu}^{2+}$ -doped (3%) q-1D AFM crystals  $\text{CsMnCl}_3 \cdot 2\text{H}_2\text{O}$  in the temperature range of 4.2–77 K. Computer simulation of an excitation walk along a 1D chain taking into account a

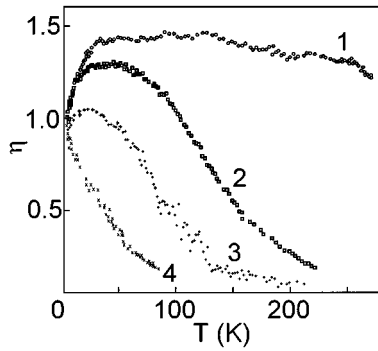


FIG. 1. Temperature dependence of the luminescence relative quantum yield of CMC crystals: undoped (1) and doped with 0.15, 1, and 3%  $\text{Cu}^{2+}$  ions (2, 3, and 4, respectively).

small hopping probability to an adjacent chain has been performed. The results were used to fit the curves of exciton emission decay kinetics of CMC crystals. An analysis is made of the  $W(T)$  and  $U(T)$  dependences in the temperature range of 4.2–237 K using also experimental data obtained earlier.<sup>3,16</sup>

## II. EXPERIMENTAL

The CMC crystals were grown from the saturated aqueous solution of  $\text{MnCl}_2 \cdot 4\text{H}_2\text{O}$  with  $\text{CsCl}$  by slow evaporation at 30 °C. CMC crystals doped with  $\text{Cu}^{2+}$  (3 mol % copper ions) were also obtained from the aqueous solution of CMC with an addition of  $\text{CuCl}_2 \cdot 2\text{H}_2\text{O}$ . The typical sizes of samples were about  $9 \times 6 \times 3 \text{ mm}^3$ . The dopant concentration of  $\text{Cu}^{2+}$  in CMC crystals was estimated by the absorption spectroscopy.<sup>3</sup>

The crystal luminescence was excited by a  $\text{N}_2$  laser. The maximum power is 5 kWt in a pulse (duration is 10 ns). A double monochromator was used as a spectral device. The emission was recorded by a photomultiplier operating in a photon counting mode. One-electron pulses from an amplifier-discriminator entered a multichannel time analyzer (0.6  $\mu\text{s}$ /channel, 4096 channels) which accumulated and averaged the emission decay curves. The experimental control and results processing were executed with a personal computer.

The sample was placed into an optical cryostat with gaseous helium. The temperature was varied from 5.2 to 77 K with an accuracy to 1 K. At 4.2 K measurements were carried out in liquid helium.

## III. RESULTS AND DISCUSSION

Figure 1 shows the effect of temperature on relative luminescence quantum yield ( $\eta$ ) of 3%  $\text{Cu}^{2+}$ -doped CMC crystals. For comparison this figure gives the dependences  $\eta(T)$  for an undoped CMC crystal and for those ones doped with 0.15 and 1%  $\text{Cu}^{2+}$  ions. For undoped crystals a rise of  $\eta$  with a temperature increase from 4.2 to 30 K is due to an additional mechanism of emission.<sup>19</sup> This mechanism is related to the pair exciton-magnon transitions. For CMC crystals doped with 1 and 0.15%  $\text{Cu}^{2+}$  the contribution from this process to the temperature dependence of  $\eta$  decreases since

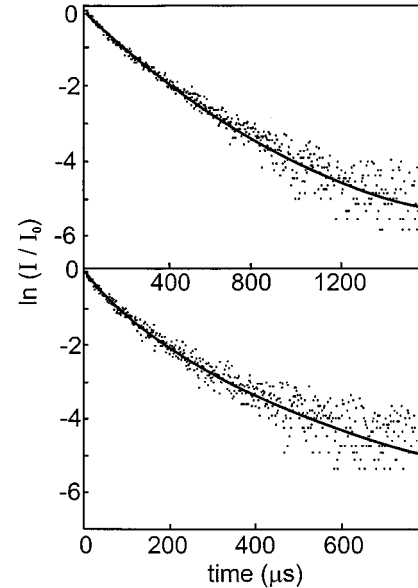


FIG. 2. The exciton emission decay kinetics of CMC crystals: doped with 3%  $\text{Cu}^{2+}$  ions at 58 K (upper curve) and 22 K (lower curve). The approximating curves are obtained as a result of computer simulation.

in these samples the emission quenching by a dopant plays more essential role. This is mostly pronounced in the  $\eta(T)$  dependence for the crystals with 3%  $\text{Cu}^{2+}$  where the luminescence quenching is observed at  $T > 4.2$  K.

The emission kinetics of 3%  $\text{Cu}^{2+}$ -doped CMC at 58 and 22 K are shown in Fig. 2. Unlike an undoped crystal or those ones doped with 0.15 and 1% copper ions, the emission decay curves are not described by the monoexponential relation in the entire temperature range studied (4.2–77 K). This points out to the fact that excitons in CMC are also trapped at very low temperatures.

### A. Computer simulation

The program algorithm for the Monte Carlo simulation of exciton migration in CMC (for more details see Ref. 16) takes into account the anisotropy peculiarities of this crystal. It is well known that a CMC crystal has strong anisotropy of the exchange integral for three crystallographic directions  $J_a : J_c : J_b = 1 : 3.3 \times 10^{-3} : 3.3 \times 10^{-4}$ .<sup>20</sup> Since the relation  $J_a > J_c > J_b$  is satisfied, we considered only the q-1D model in the 2D topology of exciton motion. The value of q-1 dimensionality  $Q$  ( $Q = W_{\text{off}}/W$ , where  $W_{\text{off}}$  and  $W$  are inter- and intrachain hopping rates, respectively) was taken as  $10^{-5}$  ( $J_a^2 : J_c^2$ ).

The following conditions were set when the simulative algorithm was developed: (a) the length of a chain segment restricted by two traps is defined by the Poisson distribution, (b) at each step an exciton can hop to a new chain with the probability equal to the parameter of  $Q$ , (c) if an exciton hops to a neighboring chain, it never comes back since the contribution from such return to the survival probability of excitons in q-1D lattice is the same as that from the hop to a new chain, (d) an exciton visiting a site neighboring to a trap

TABLE I. Exciton hopping and trapping rates in CMC obtained using Monte Carlo simulation.

Sample	Temperature K	Rate $10^6 \times s^{-1}$	
		$W$	$U$
3% Cu <sup>2+</sup>	4.2	3.2	0.09
	15	4.0	0.11
	22	4.4	0.12
	42	6.1	0.15
	58	$1.0 \times 10^1$	0.20
	77	$5.7 \times 10^1$	0.50
1% Cu <sup>2+</sup>	77	$5.2 \times 10^1$	0.5
	99	$8.0 \times 10^1$	0.6
	123	$4.2 \times 10^2$	1.4
	145	$3.5 \times 10^3$	1.8
0.15% Cu <sup>2+</sup>	159	$4.0 \times 10^3$	3.1
	150	$4.2 \times 10^3$	3.1
	169	$9.8 \times 10^3$	4.8
	179	$1.5 \times 10^4$	7.0
	218	$3.9 \times 10^4$	14.0
	225	$4.4 \times 10^4$	11.0
	237	$3.4 \times 10^4$	17.0

is captured with the probability defined by the expression  $\lambda/(\lambda+1) = U/(U+W)$  ( $\lambda = U/W$  is the trap efficiency) or returns back.

After each step the total number of untrapped excitons was computed. Thus, averaging over all the excitons (their number varied from  $10^4$  to  $10^5$ ) we obtained the decay law of survival probability. To account for the spontaneous decay of excitons this probability was multiplied by the exponential expression with the characteristic exciton lifetime. This lifetime ( $\tau$ ) was defined from the decay curve of undoped CMC crystals.

The simulative data obtained using the present algorithm were compared with the experimental decay curves. At fitting two parameters— $W$  and  $U$ —have been varied. The best fitting is shown in Fig. 2 for two temperatures (22 and 58 K). The agreement between the simulated and experimental decay curves is good. The values of  $W$  and  $U$  obtained for CMC doped with 3% Cu<sup>2+</sup> at 4.2–77 K are presented in Table I. In this table the values of  $W$  and  $U$  for CMC doped with 1 and 0.15% Cu<sup>2+</sup> are given too. These experimental data were obtained earlier<sup>3</sup> and used for development of an exciton migration model in CMC over the whole temperature range.

The temperature dependences of  $W$  and  $U$  are shown in Fig. 3. The semi-log scale is chosen to see whether the approximation of experimental dependence by the Arrhenius law is applicable. As can be seen from the figure neither hopping nor trapping rates can be described by a straight line in the entire temperature range. Taking into account these temperature dependences of  $W$  and  $U$  we assume that excitons not only overhop the potential barriers between Mn<sup>2+</sup>-Mn<sup>2+</sup> and Mn<sup>2+</sup>-Cu<sup>2+</sup> sites but also tunnel through them. At low temperatures the latter process begins to play an essential role in the energy migration. These barriers for excitons are formed due to the exciton-phonon coupling (Mn<sup>2+</sup>-Mn<sup>2+</sup>) or to the exciton-impurity interaction

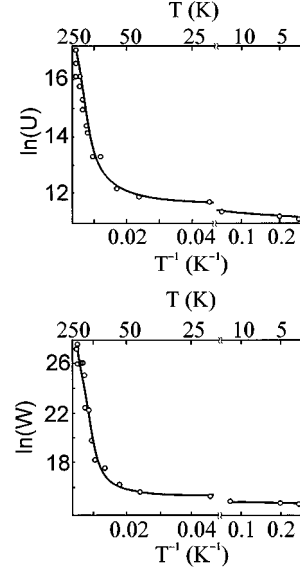


FIG. 3. Temperature dependences of the hopping (upper curve) and trapping (lower curve) rates of an exciton in CMC crystals. Approximating curves are calculated by Eq. (1).

(Mn<sup>2+</sup>-Cu<sup>2+</sup>). Besides, exciton migration along a chain decreases due to AFM ordering which should be manifested in CMC below  $T \approx 30$  K.<sup>21</sup>

### B. Exciton tunneling

The role of exciton tunneling through potential barriers between Mn<sup>2+</sup> and Cu<sup>2+</sup> ions was considered earlier.<sup>22</sup> An account of this process has given the possibility to describe the temperature dependence of  $U$  over the range of 77–237 K. Unlike  $U(T)$ , the  $W(T)$  dependence has not displayed considerable deviations from the Arrhenius law within the same temperature range.

When the temperature range of the experiment was extended down to 4.2 K, the form of  $W(T)$  dependence turned out to be similar to that of  $U(T)$  (Fig. 3). As was mentioned above the approximation of this dependence is impossible by the Arrhenius law.

Let us take into account the tunneling processes and use the same form of  $W(T)$  as that of  $U(T)$  in Ref. 22:

$$W(T) = W_0 B_W(T) K_W(T). \quad (1)$$

Here  $W_0$  is the normalization constant

$$B_W(T) = \frac{1}{T} \int_0^\infty Q(E) \exp\left(-\frac{E}{k_B T}\right) dE, \quad (2)$$

$K_W(T)$  is the spin-correlation factor (will be considered further).

$Q(E)$  is a function of the interstitial hop probability:<sup>22,23</sup>

$$Q(E) = \begin{cases} \exp\left(-\frac{2}{h} \int_{x_1}^{x_2} \sqrt{2m(\mathbf{U}(x) - E)} dx\right) & \text{for } E < \Delta_W, \\ 1 & \text{for } E > \Delta_W. \end{cases} \quad (3)$$

$h$  is the Planck constant,  $m$  is the exciton effective mass,  $\Delta_W$  is the barrier energy,  $x$  is a running coordinate along a chain,  $x_1$  and  $x_2$  are the roots of equation  $\mathbf{U}(x)=E$ .

The expression (3) was obtained in the quasiclassical approximation<sup>22,23</sup> of tunneling of waves. The exciton localization in CMC leads to the production of an additional factor which is insignificant in our case since the function  $W(T)$  is determined up to a constant factor  $W_0$ .

Let us consider the parabolic profile of the potential barrier  $\mathbf{U}(x)=(\Delta_W/l^2)(l^2-x^2)$  for which integration (2) may be carried out in the explicit form

$$B_W(T) = \frac{T \exp(-\Delta_W/k_B T) - T_t \exp(-\Delta_W/k_B T_t)}{T - T_t}, \quad (4)$$

$$T_t = \frac{h}{k_B \pi l} (\Delta_W/2m)^{1/2}. \quad (5)$$

$l$  is the barrier width which is considered to be equal to half the site-to-site distance  $a$  (in CMC  $a=4.53 \text{ \AA}$ ). Let us introduce the exciton bandwidth  $E_0$  with regard for the condition  $m=h^2/(2\pi)^2 E_0 a^2$ . Using the relation between bandwidth  $E_0$  and the exchange integral  $J_f$  in the photoexcited state along the chains direction ( $E_0=ZJ_f S_f$ ,  $S_f=S-1$ ,  $S$  is the  $\text{Mn}^{2+}$  ions spin in the ground state,  $S_f$  in the photoexcited one,  $Z=2$  is the number of nearest magnetic neighbors in a chain), one can obtain

$$T_t = 2 \frac{\sqrt{J_f S_f \Delta_W}}{k_B}. \quad (6)$$

Fitting of the experimental dependence (Fig. 3) was carried out by calculated curves using Eq. (1). As a result, we obtained  $\Delta_W \sim 1300 \text{ cm}^{-1}$  and  $J_f \approx 0.7 \text{ cm}^{-1}$  which corresponds to  $m \sim 10^3 m_e$  where  $m_e$  is the free-electron mass and  $T_t \sim 100 \text{ K}$ .

$T_t$  is the temperature below which quantum tunneling effects begin to manifest themselves. Under the condition  $\Delta_W \gg k_B T_t$  the temperature  $T_t$  corresponds to the maximum curvature of line (4). In the low-temperature range  $T \ll T_t$ , the factor  $B_W(T)$  is determined exclusively by tunneling processes and is proportional to  $\exp(-\Delta_W/k_B T) = \exp(-s/h)$  where  $s = \pi l (2m \Delta_W)^{1/2}$  is the action. At  $h \rightarrow 0$  (or  $T_t \rightarrow 0$ ), Eq. (4) transforms to the Arrhenius form.

In the high-temperature region  $T \gg T_t$ , the temperature dependence of  $B_W$  is of the Arrhenius-law-type —  $B_W(T) \sim \exp(-\Delta_W/k_B T)$  with the renormalization  $\Delta_W: \Delta_W \rightarrow \Delta_W - k_B T_t$ .

We have considered more general type of the potential barriers profile ( $\mathbf{U}(x) = \Delta_W [1 - (x/l)^p]$  where  $0 < p < \infty$ ), the parameter  $p$  has been also varied at fitting the experimental dependence  $W(T)$ . The calculation gives the best fit to the experimental data at  $p=1.8$  which is close to the parabolic barrier profile.

### C. The role of the magnetic subsystem ordering

The influence of magnetic subsystem ordering on exciton transport is described by the factor  $K_W(T)$  in (1).  $K_W(T) = 2 \langle |(\vec{\sigma}_n^+ \cdot \vec{\sigma}_{n+1})| \rangle$  is the correlation function of spins in a chain;  $\vec{\sigma}_n^+$ ,  $\vec{\sigma}_{n+1}$  are the vector operators of creation and

annihilation of optical excitations.<sup>24</sup> The operator  $(\vec{\sigma}_n^+ \cdot \vec{\sigma}_{n+1})$  corresponds to the process of intersublattice exciton movement and describes the Davydov splitting.<sup>25</sup> The  $K_W(T)$  dependence for an antiferromagnetic ordering in chains can be obtained in the following way. Using the unitary transformation of the operators  $\vec{\sigma}_n^+$  and  $\vec{\sigma}_{n+1}$  let us go over from the coordinate system connected with the crystallographic axes to the local system connected with spins of the nearest sites “ $n$ ” and “ $n+1$ .” The scalar product  $(\vec{\sigma}_n^+ \cdot \vec{\sigma}_{n+1})$  is transformed from the crystallographic axes  $X, Y, Z$  to the new ones  $\xi_n, \eta_n$ , and  $\zeta_n$  (the  $\zeta_n$  axis is chosen along the direction of a spin in the position “ $n$ ”) and then to the linear combination of  $\xi_n$  and  $\eta_n$ :  $\xi_n + i\eta_n$  and  $\xi_n - i\eta_n$ . Then the factor  $\cos^2(\theta/2)$  at  $\sigma_{n,-}^+ \cdot \sigma_{n+1,-}$  which corresponds to the optical transition  $|S-1, S-1; S, S\rangle \rightarrow |S, S; S-1, S-1\rangle$  describes the Davydov splitting and the resonance hop of optical excitation from  $n$  to  $n+1$  site. Here  $\theta$  is the angle between spins  $n$  and  $n+1$  from the opposite sublattices.

At zero temperature in strictly ordered AFM structures  $\theta = \pi$  and the factor  $\cos^2(\theta/2)$  is equal to zero which corresponds to the absence of Davydov splitting in *collinear* AFM crystals.<sup>26</sup> This additional (spin) forbiddenness on the Davydov splitting and on the intersublattice resonance hopping of optical excitation is partially removed even at zero temperature under break of the AFM ordering. Such a break can be induced by external magnetic fields.<sup>26,27</sup>

To calculate  $K_W(T)$  at finite temperatures it is necessary to average the factor  $\cos^2(\theta/2)$  over the thermodynamic ensemble of spins in a chain:

$$K_W(T) = \left\langle \cos^2\left(\frac{\theta}{2}\right) \right\rangle = \frac{1}{2} [1 + \langle \cos(\theta) \rangle] = \frac{1}{2} \left( 1 + \frac{\langle S_n S_{n+1} \rangle}{S^2} \right), \quad (7)$$

where  $\langle \dots \rangle$  denotes averaging.

The correlation function (7) was calculated<sup>22</sup> using the molecular field approximation:

$$K(T) = \frac{1}{2} \left( 1 - \left[ \frac{(1-z^{2S+2}) - (1+1/S)z(1-z^{2S})}{(1-z)(1-z^{2S+1})} \right]^2 \right) \quad (8)$$

$z = \exp(-\varepsilon_{\max}/k_B T)$ , with the magnon bandwidth in the ground state being about  $\varepsilon_{\max} = 25 \text{ cm}^{-1}$  for CMC.<sup>28</sup>

The factor  $K_W(T)$  is the increasing function of a temperature. The vicinity of  $\varepsilon_{\max}/k_B$  is the region of the largest change in  $K_W(T)$ . At  $T > 2\varepsilon_{\max}/k_B$   $K_W(T)$  is practically independent of temperature and is approximately equal to 1/2 (see the inset in Fig. 4).

The temperature dependence  $U(T)$  can be represented as follows:

$$U(T) = U_0 B_U(T) K_U(T).$$

The factor  $B_U(T)$  in the expression for  $U(T)$  is of the same form as Eq. (1) and differs by the barrier energy  $\Delta$  only ( $\Delta_U$  is about  $800 \text{ cm}^{-1}$ ). More essential differences are related to the spin-correlation factor  $K_U$ . First of all, a possible difference between spin values of host  $S$  and impurity  $S'$

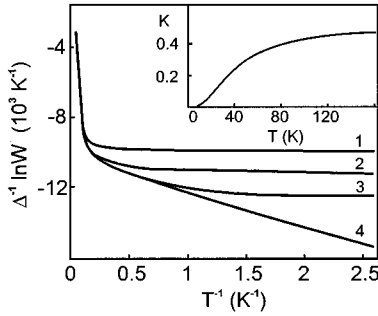


FIG. 4. Theoretical temperature dependences of the exciton hopping rate in CMC crystals under different degrees of the spin forbiddenness. Curve 1 corresponds to the spin-correlation factor being a constant [Eq. (4)]; the spin-correlation factor in the isotropic form is taken into consideration [curve 4, Eq. (7)]; both isotropic and anisotropic [Eq. (9)] resonance terms are taken into account (curves 2,3). The ratio of amplitudes of the anisotropic part of interaction and isotropic one 0.1 and 0.01 corresponds to curves 2 and 3, respectively. In the inset the temperature dependence of the spin-correlation factor (9) is presented.

ions should be taken into account. The second important difference between hopping and trapping is that the exciton trapping is the nonresonance phenomenon and optical transitions among all sublevels of multiplet should be estimated [but not only  $|S' - 1, S' - 1; S, S\rangle \rightarrow |S', S'; S - 1, S - 1\rangle$ ,  $S'$  is the impurity ion spin].

It may be shown that even at low temperatures and without AFM ordering break of the spin forbiddenness is not strict for  $W(T)$  as well. It becomes clear if anisotropic terms in the expression for  $K_W$  are considered, i.e.,  $K_W$  is represented in the form

$$K_W = 2 \left\langle \left| \sum \alpha_i \vec{\sigma}_{n,i}^+ \cdot \vec{\sigma}_{n+1,i} \right| \right\rangle \quad (i=x,y,z) \quad (9)$$

with different  $\alpha_i$  which is allowed by the symmetry of a biaxial AFM crystal CMC. These considerations are also related to  $U(T)$ .

Besides the static mechanisms of partial removal of the spin forbiddenness from the low temperature exciton motion, the dynamic ones can occur. In particular, it concerns the excitation of spin waves owing to the phonons relaxation. Probably, this mechanism is especially efficient when exciting light generates phonons together with optical excitations [in the present work we do not consider the effect of non-equilibrium phonons on the exciton emission decay since the time of their relaxation is presumed to be shorter than the time resolution of our registration setup ( $10^{-5} - 10^{-6}$  s)] (as in our case).

Spin correlations described by the factor  $K_W$  manifest themselves in the low temperature range  $T \ll \varepsilon_{\max}/k_B \sim 35$  K (Fig. 4). Under the strict spin forbiddenness the function  $\ln(W(T^{-1}))$  decreases with a temperature lowering. An incline is determined by  $\varepsilon_{\max}$ . If the forbiddenness is not strict then the curve  $\ln(W(T^{-1}))$  tends to a plateau similar to the experimental dependence (Fig. 3). At moderate and high temperatures the magnetic subsystem has practically no in-

fluence on the exciton transport, so far as the maximum magnon energy is much less than the energy of exciton-phonon interaction ( $\varepsilon_{\max} \ll \Delta$ ).

#### D. Is the exciton transport coherent in CMC at low temperatures?

In the present work we have used an incoherent model of the exciton motion to fit experimental curves both at high temperatures and close to the helium ones. With reason an incoherent model may be applied to the exciton transport description at  $T > 30$  K but its application at lower temperatures is not evident *a priori*. Unfortunately, up to now special investigations of the exciton transport topology in CMC have not been carried out. In the present state of affairs the only general speculations may be used for a model choice at low temperatures. We adduce some arguments in favor of an incoherent model in this crystal even near helium temperatures.

(i) The temperature dependence of exciton mobility in q-1D AFM's appreciably differs from that of other (e.g., molecular) crystals (see, for instance, the review, Ref. 29). In molecular crystals at a temperature decrease from 300 to 60–100 K the diffusion coefficient drops and at  $T < 30 - 40$  K, it rises. An increase of mobility in these crystals at low temperatures is attributed to a change of the exciton motion from incoherent to coherent. The slowed-down exciton transport in CMC with a temperature decrease is reflected in a smooth increase of  $\eta$  for doped samples (Fig. 1). It is also exhibited in the behavior of emission decay kinetics of doped crystals. At a temperature decrease the decay curve in the semi-log scale becomes straight more and more and approaches the monoexponential form with the lifetime close to that of an undoped crystal. It can be assumed that at a temperature decrease only parameter  $U$  is reduced. However, under these conditions we failed in fitting the experimental decay curves (varying  $U$  only). Certainly, a decrease of trapping in CMC at low temperatures can be associated with barriers for excitons caused by residual impurity. However, the concentration of such impurity should exceed that of the ions forming traps for excitons (in our case above 3%) to block excitons in cages. Such a concentration of residual impurities detected in CMC after special purification is unlikely. Moreover, on this assumption the emission decay kinetics should consist of two parts: a fast drop of the intensity characteristic of excitons in cages with traps and then the slow one with the lifetime of an undoped crystal due to the emission from cages without traps. The character of exciton decay in CMC at low temperatures appreciably differs from that shown in Fig. 2. Thus, as it follows from the temperature dependence of  $\eta$  and  $W$  in this crystal, the exciton mobility in CMC does not increase at  $T < 30 - 40$  K, as is the case of coherent excitons,<sup>29</sup> but decreases.

(ii) CMC is AFM with a fairly strong exciton-phonon interaction.<sup>5</sup> As a consequence, a broad structureless phonon sideband and a weak phononless line are observed in the luminescence spectrum of this crystal. Such interaction will impede the propagation of the coherent exciton wave in a crystal.

(iii) AFM ordering of spins in chains makes the coherent exciton transport in q-1D collinear AFM crystals with AFM

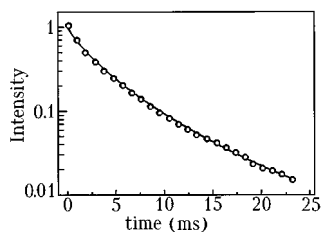


FIG. 5. Decay curve of exciton emission calculated by using Huber's theory (solid line). The calculated decay curve is obtained at  $\Gamma=1.65 \text{ ms}^{-1}$  and  $\alpha=0.105 \text{ ms}^{-1}$  ( $\Gamma$  and  $\alpha=1/\tau$  and their values were taken from Ref. 30). Circles present the result of the Monte Carlo simulation.

spins ordering practically unreal. Indeed, unlike magnons, optical excitations in *collinear* AFM's spread within a magnetic sublattice (i.e., between ions with parallel spins only). These are either ions from different chains or ions following the nearest neighbors (i.e., separated by the distance of  $2a$ ). However, the corresponding exchange interactions are too weak in CMC to ensure the coherent exciton transport.

(iv) No doubt, doped ions break coherence of the exciton motion. This break is more essential when the dopant concentration is higher and the interaction leading to the coherent motion is weaker. In the CMC crystals studied the dopant concentration is sufficiently high (1–3%) and the exchange interactions between nearest neighbors is weak (a few  $\text{cm}^{-1}$ ). It is not inconceivable, that a dopant ion may slightly change the energy structure of the host near an impurity. In this case a degree of the local structure deformation near a dopant will also play an important role in a break of coherence.

Thus, in CMC excitons are most likely incoherent even at low temperatures, at least, when  $T > T_N$  (4.89 K). Finally, we tried to elucidate whether the adjustment of experimental curves of the exciton emission decay can serve as a basis for a conclusion about the topology of exciton motion. With this end in view, the exciton decay curves obtained using two different models were compared. The computer simulation of trapping of 1D incoherent excitons and the above Huber's coherent model<sup>29</sup> were used. To move this problem closer to our objects, we scanned the Huber's calculative curves from Ref. 30. As shown in Fig. 5, the simulative data gave a good fit to the calculated decay curve. As a result, we evaluated the hopping and trapping rates of excitons in the  $\text{CsMnCl}_3 \cdot 2\text{D}_2\text{O}$  crystal at 2 K ( $W=6 \times 10^6 \text{ s}^{-1}$ ,  $U=10^5$

$\text{s}^{-1}$ ). These rates are close to the values of  $W$  and  $U$  defined for CMC doped with 3%  $\text{Cu}^{2+}$  at 4.2 K (see Table I).

We have not studied specially the range of variable of  $W$  and  $U$  where both the coherent and incoherent models result in practically identical decay curves. However, coincidence of the curves (Fig. 5) obtained using different models admits to make a conclusion that kinetic decay curve alone does not always enable one to choice between two models of exciton migration. In our opinion, it is necessary to carry out special investigations to arrive at the finite conclusion about the type of exciton motion at helium temperatures.

#### IV. CONCLUSION

The temperature dependence of the exciton hopping rate in a CMC crystal and that of trapping by  $\text{Cu}^{2+}$  ions from 4.2 to 237 K are not described only by the Arrhenius law. Deviations from this law are due to exciton tunneling through the potential barrier both at a hop between  $\text{Mn}^{2+}$ - $\text{Mn}^{2+}$  ( $\Delta_W=1300 \text{ cm}^{-1}$ ) and at a hop between  $\text{Mn}^{2+}$ - $\text{Cu}^{2+}$  ( $\Delta_U=800 \text{ cm}^{-1}$ ). An analysis of the dependence  $W(T)$  showed that in CMC below  $T=100 \text{ K}$  tunneling plays the predominant role in the exciton migration.

The lowering probability for excitons to be trapped in CMC under a temperature decrease from room to helium (as may be inferred from the temperature dependence of a relative quantum yield of doped crystals) and the shape of  $W(T)$  dependence indicate that in this crystal excitons are not coherent in the entire temperature range studied. This is due to a fairly strong exciton-phonon interaction in a crystal as well as to the spin forbiddenness of exciton migration manifesting itself in CMC mainly at  $T < 30 \text{ K}$ .

Fitting of the luminescence decay curves of  $\text{CsMnCl}_3 \cdot 2\text{D}_2\text{O}$  crystals by the calculated dependences obtained in a model of both coherent and incoherent excitons is quite satisfactory. The emission decay curves calculated using the Huber's model of coherent excitons and those simulated in the model of hopping excitons are, in fact, coincident. Thus, one cannot always succeed in the determination of the type of exciton transport (coherent or incoherent) from the emission decay curves alone.

#### ACKNOWLEDGMENTS

We are grateful to Dr. I. Kachur and Dr. A. Kazachkov for the CMC crystals growing. This work was partially supported by the International Science Foundation Grant (No. K5i100).

<sup>1</sup>R.A. Auerbach and G. McPherson, *Phys. Rev. B* **33**, 6815 (1986).

<sup>2</sup>R. Knochenmuss and H.U. Gudel, *J. Chem. Phys.* **86**, 1104 (1987).

<sup>3</sup>V.V. Eremenko, V.A. Karachevtsev, A.R. Kazachkov, V.V. Shapiro, and V.V. Slavin, *Phys. Rev. B* **49**, 11 799 (1994).

<sup>4</sup>G. McPherson, Y.Y. Waguespack, T.C. Vanoy, and W.J. Rodriguez, *J. Chem. Phys.* **92**, 1768 (1990).

<sup>5</sup>W. Jia, R.T. Brundage, and W.M. Yen, *Phys. Rev. B* **27**, 41 (1983).

<sup>6</sup>H. Yamamoto, D.S. McClure, C. Marzocco, and M. Waldman, *Chem. Phys.* **22**, 79 (1977).

<sup>7</sup>Y. Balagurov and V.G. Vaks, *Zh. Éksp. Teor. Fiz.* **65**, 1939 (1973) [*Sov. Phys. JETP* **38**, 968 (1974)].

<sup>8</sup>R.D. Wieting, M.D. Fayer, and D.D. Dlott, *J. Chem. Phys.* **69**, 1996 (1978).

<sup>9</sup>J. Klafter and R. Silbey, *J. Chem. Phys.* **72**, 849 (1980).

<sup>10</sup>P. Grassberg and I. Procaccia, *J. Chem. Phys.* **77**, 6281 (1982).

<sup>11</sup>B. Movaghar, G.W. Sauer, and D. Wurtz, *J. Stat. Phys.* **27**, 473 (1982).

<sup>12</sup>V.M. Kenkre and P.E. Parris, *Phys. Rev. B* **27**, 3221 (1983).

<sup>13</sup>A. Blumen, J. Klafter, and G. Zumofen, *J. Chem. Phys.* **82**, 3198 (1985).

- <sup>14</sup>A.I. Onipko, L.I. Malysheva, and I.V. Zozulenko, *Chem. Phys.* **121**, 99 (1988).
- <sup>15</sup>W.J. Rodriguez, M.F. Herman, and G. McPherson, *Phys. Rev. B* **39**, 13 187 (1989).
- <sup>16</sup>V.A. Karachevtsev, I.A. Levitsky, and V.V. Slavin, *J. Chem. Phys.* **103**, 2656 (1995).
- <sup>17</sup>X.K. Wu, W.M. Dennis, W.M. Yen, W. Jia, and D.L. Huber, *J. Lumin.* **58**, 361 (1994).
- <sup>18</sup>M.D. Fayer, in *Spectroscopy and Excitation Dynamics of Condensed Molecular Systems*, edited by V.M. Agranovich and R.M. Hochstrasser (North-Holland, Amsterdam, 1983), p. 185.
- <sup>19</sup>V.V. Eremenko, V.A. Karachevtsev, A.R. Kazachkov, V.V. Shapiro, and V.V. Slavin, *Solid State Commun.* **87**, 1027 (1993).
- <sup>20</sup>H. Nashihara, W.J.M. de Jonge, and T. de Neef, *Phys. Rev. B* **12**, 5325 (1975).
- <sup>21</sup>J. Skalyo, G. Shirane, S.A. Friedberg, and H. Kobayashi, *Phys. Rev. B* **2**, 1310 (1970).
- <sup>22</sup>V.V. Eremenko, V.A. Karachevtsev, V.V. Slavin, and V.V. Shapiro, *Low Temp. Phys.* **19**, 908 (1993) [*Low Temp. Phys.* **19**, 1277 (1993)].
- <sup>23</sup>L.D. Landau and E.M. Lifshitz, *Quantum Mechanics* (Pergamon, New York, 1965).
- <sup>24</sup>T. Fujiwara and Y. Tanabe, *J. Phys. Soc. Jpn.* **32**, 912 (1972).
- <sup>25</sup>A.S. Davydov, *Theory of Molecular Excitons* (Plenum, New York, 1971).
- <sup>26</sup>V.P. Novikov, V.V. Eremenko, and V.V. Shapiro, *J. Low. Temp. Phys.* **10**, 95 (1973).
- <sup>27</sup>M. Igarashi, F. Tusuruoka, H. Tanaka, I. Ajiro, and K. Nagata, *J. Phys. Soc. Jpn.* **60**, 236 (1991).
- <sup>28</sup>J. Skalyo, G. Shirane, S.A. Friedberg, and H. Kobayashi, *Phys. Rev. B* **2**, 4632 (1970).
- <sup>29</sup>R. Silbey, in *Spectroscopy and Excitation Dynamics of Condensed Molecular Systems* (Ref. 18), p. 5.
- <sup>30</sup>D.L. Huber, *Phys. Rev. B* **45**, 8947 (1992).